Soil Use and Management

WILEY | BRITISH SOCIETY OF SOIL SCIENCE

RESEARCH ARTICLE OPEN ACCESS

Spatial Variation of Acidic Sodic Soils in High-Andean Environments and Theoretical Estimation of Gypsum Requirement

Kenyi Quispe[1] | Nilton Hermoza[1] | Sharon Mejia[1] | Elvis Ccosi[2] | Dalmecio Miranda[2] | Luz Choquechambi[2] | Katherin Choquehuanca[2] | Edgar Carrasco[2] | Néstor Cuellar-Condori[2]

[1]Dirección de Servicios Estratégicos Agrarios, Instituto Nacional de Innovación Agraria (INIA), Lima, Peru | [2]Dirección de Servicios Estratégicos Agrarios – INIA, Puno, Peru

Correspondence: Kenyi Quispe (k.quispe1008@gmail.com)

Received: 25 September 2025 | **Revised:** 15 May 2026 | **Accepted:** 3 June 2026

Keywords: acidic sodic soils | clay dispersion | exchangeable sodium percentage | soil quality index | spatial analysis

ABSTRACT

High-Andean forage systems are characterized by extensive management of cultivated forages, primarily through rotation of forage oats (*Avena sativa*) and alfalfa (*Medicago sativa*), under marginal edaphoclimatic conditions. Within this context, soil sodicity severely constrains the productivity of these systems in the districts of Ayaviri and Macarí, Melgar Province, Peru. However, spatially explicit information on gypsum requirements (GR) for sodic-soil reclamation remains unavailable. To address this gap, this study aimed to: (i) develop a weighted Soil Quality Index (SQIw) for sodic soils, (ii) delineate sodicity-affected areas across districts, soil classes and environmental conditions and (iii) generate high-resolution maps of gypsum requirements using regression kriging (RK). A total of 1273 soil samples were analysed in high-altitude areas of Ayaviri and Macarí. Key sodicity-related variables included exchangeable sodium percentage (ESP), clay flocculating charge and Modified Soil-Adjusted Vegetation Index (MSAVI) selected through Pearson correlation and principal component analysis to construct the SQIw, while regression kriging was used to generate spatially explicit gypsum requirement maps. Results showed wide variability in pH and ESP, reflecting heterogeneous sodicity conditions across the study area, with Macarí presenting higher soil quality (SQIw = 0.61) than Ayaviri (SQIw = 0.44). Sandy loam soils and acid saline–sodic soils exhibited the greatest vulnerability. Regression kriging achieved high predictive accuracy for GR estimation (R^2 = 0.97 in Ayaviri; R^2 = 0.85 in Macarí), enabling precise delineation of priority intervention zones. The resulting GR maps provide a robust basis for site-specific gypsum application, improving amendment efficiency, reducing unnecessary costs and supporting sustainable sodicity management in vulnerable High-Andean agroecosystems.

1 | Introduction

Soil quality underpins the sustainability of High-Andean forage systems, where marginal edaphoclimatic conditions and limited resources constrain production. In Melgar Province (Puno, Peru), forage production based on oat (*Avena sativa*) and alfalfa (*Medicago sativa*) sustains livestock feeding and the local economy; between 2018 and 2022 livestock numbers and milk production increased notably (INEI 2023). These systems are predominantly managed under extensive and semi-extensive regimes, relying upon natural pastures and cultivated forages to maintain productivity and local food security. Rotation of forage oat with alfalfa enhances soil structure, nutrient retention and erosion control at elevations above 3000 m a.s.l., while alfalfa additionally contributes nitrogen fixation and high feed value (Bernal 2013; Programa de Desarrollo Productivo Agrario Rural 2018; Xu et al. 2024).

Notwithstanding these benefits, establishment and productivity of forage species are frequently limited by soil salinity and, in particular, sodicity. Sodic soils—commonly defined by elevated exchangeable sodium percentage (ESP > 15%) and sodium adsorption ratio (SAR > 13)—promote clay dispersion, weaken aggregate stability and reduce infiltration and plant-available water and nutrients (Daba and Qureshi 2021). Such physico-chemical constraints impose both osmotic and ionic stresses on crops, with documented yield penalties in sensitive species including alfalfa (Anderson et al. 2023; Bai et al. 2024). Global assessments point to an extensive and growing area affected by sodium accumulation (FAO 2024), while in the Peruvian Altiplano sodicity is frequently associated with poor drainage, saline groundwater and irrigation regimes that favour salt accumulation in fine-textured layers (Revollo 2001; Banks et al. 2004; Hervé et al. 2002).

In the High-Andean Altiplano, soils frequently exhibit complex acid–sodic conditions, where sodicity can develop even at relatively low exchangeable sodium percentage (ESP) values (≈6%), particularly under conditions of low base saturation, limited buffering capacity and episodic salinization (Cuellar-Condori et al. 2026). Acid–sodic soils are of increasing concern because structural degradation, clay dispersion and reduced hydraulic conductivity may occur before classical sodicity thresholds are reached, thereby complicating their diagnosis and management. Despite their agronomic relevance, studies on acid–sodic soils remain limited both in the Andes and globally, particularly regarding their spatial variability and management thresholds (Rengasamy 2002; Qadir and Schubert 2002; Hengl et al. 2017).

Crucially, labelling a soil as 'sodic' using a single chemical indicator does not capture the spatial heterogeneity nor the functional degree of degradation that constrain management decisions. The agronomic consequences of sodicity stem from interacting chemical, physical and climatic controls; soils with similar ESP or SAR may nevertheless differ markedly in aggregate stability, hydraulic conductivity and biological performance. In this regard, composite, multivariate assessments provide a more informative characterization of soil condition (Poma-Chamana et al. 2025). The Soil Quality Index for Sodicity (SQIw) proposed here synthesizes structural (texture and bulk density), chemical (ESP, ECEC, exchangeable Ca^{2+}, and Mg^{2+}) and, where available, biological indicators (vegetation indices) into a single interpretable metric that reflects both severity and resilience. By integrating these attributes, the SQIw furnishes a consistent framework for linking sodicity severity to gypsum requirement (GR) at spatial scales relevant for management and prioritisation. Previous studies indicate that weighted multivariate soil quality indices can effectively discriminate recovery following reclamation and are useful for monitoring temporal and spatial changes in degraded soils (Bedolla-Rivera et al. 2022).

The spatial variability of sodicity poses a major challenge for sustainable pasture management because zones of contrasting severity demand different amendment rates and management strategies (Yang et al. 2016). Geographic information systems (GIS) and geostatistical techniques are therefore essential for characterising this variability and for producing spatially explicit decision-support products (Quispe et al. 2025). Regression kriging (RK), which couples deterministic regression on ancillary covariates (remote sensing, topography, and soil maps) with kriging of residuals, is particularly effective when relevant auxiliary data are available; RK typically improves prediction accuracy and reduces estimation error relative to purely interpolation-based approaches (Hengl et al. 2007; Burrough et al. 2015). Applied studies have used geostatistical methods to map ESP, SAR and gypsum requirement and to delineate management zones, demonstrating that spatially explicit GR maps can substantially reduce over- and under-application of amendments compared with blanket treatments (Roberton et al. 2020). Nevertheless, the joint application of geostatistics and multivariate soil quality indices for sodicity assessment remains under-explored in cold, semi-arid mountain systems such as the Andean Altiplano.

Gypsum ($CaSO_4 \cdot 2H_2O$) is widely recommended for reclamation of sodic soils because Ca^{2+} replaces Na^+ on the exchange complex, thereby reducing clay dispersion and promoting aggregation and hydraulic recovery. The relative effectiveness of gypsum derives from the higher selectivity and smaller hydrated radius of Ca^{2+} compared with Na^+, and from gypsum's solubility characteristics that facilitate sodium displacement under leaching conditions (Havlin et al. 2016; Bello et al. 2021). Despite this, robust, spatially explicit estimates of gypsum requirement and of the production losses attributable to sodicity are limited for High-Andean pastures, constraining evidence-based prioritisation and the design of locally adapted reclamation policies at district scale.

We hypothesized that: (i) acid–sodic conditions in the High-Andean Altiplano develop at lower ESP thresholds than traditionally recognized, driven by low base saturation and limited buffering capacity; (ii) a weighted, multivariate Soil Quality Index (SQIw) can effectively differentiate functional degradation levels across heterogeneous landscapes; and (iii) regression kriging, integrated with edaphic and remote-sensing covariates, will yield spatially explicit gypsum requirement maps that outperform uniform blanket recommendations. This study addresses a critical knowledge gap, as diagnostic frameworks and spatially explicit management tools for acidic sodic soils remain severely underrepresented globally, particularly in cold, semi-arid mountain systems.

Accordingly, this study aims to: (i) develop a Soil Quality Index oriented to sodicity (SQIw); (ii) delineate the spatial extent of sodicity-affected areas across districts, soil classes and landscape units; and (iii) generate high-resolution maps of gypsum requirement (GR) using regression-kriging to provide a quantitative basis for site-specific management in High-Andean forage systems.

2 | Materials and Methods

2.1 | Study Area

The study was conducted in the districts of Ayaviri and Macarí, Melgar Province, Puno Region, within the Peruvian

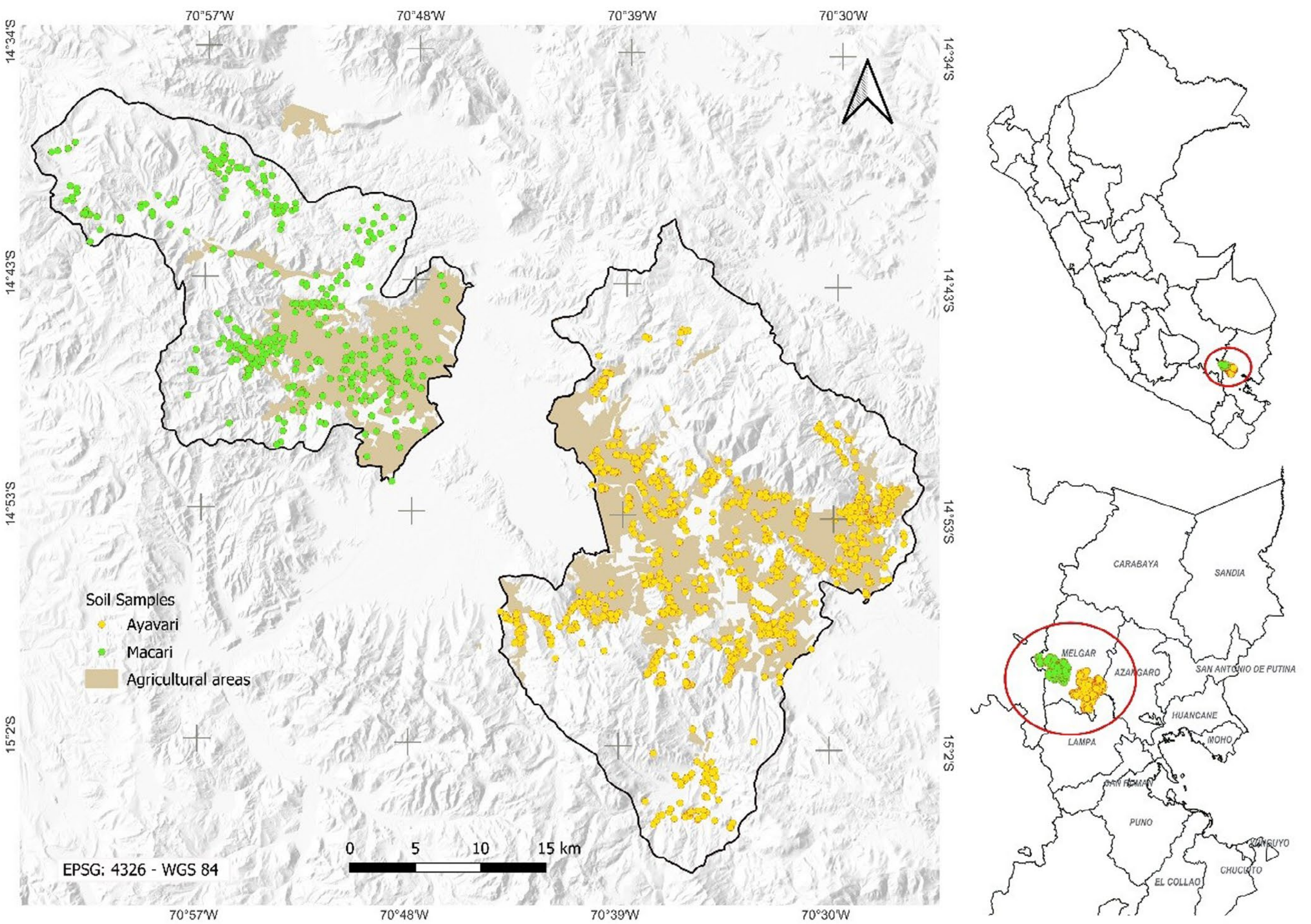

FIGURE 1 | Geographic location of the study area and spatial distribution of the 1,273 soil sampling sites across the districts of Ayaviri and Macarí, Melgar Province, Puno, Peru.

highlands (Figure 1). The total study area covers 1381.08 km^2, comprising 855.79 km^2 in Ayaviri and 525.29 km^2 in Macarí. The area has an average annual precipitation of 791.5 mm, mean relative humidity of 60.9%, and temperatures ranging from −5.3°C (minimum) to 20.5°C (maximum) (Figure S1; Fick and Hijmans 2017). Alluvial slopes predominate (58%), with life zones corresponding to Subtropical Lower Montane Moist Forest (64%) and Subtropical Subalpine Very Humid Páramo (36%). Soils are mainly Cambisols, followed by Chernozems and Phaeozems (IUSS Working Group WRB 2024). The principal crops are alfalfa '*Medicago sativa*' and oats '*Avena sativa*' (Figure S2).

2.2 | Soil Sampling

Soil sampling followed the model of Havlin et al. (2016), where each sample represented a homogeneous area defined by slope, soil texture/colour, crop type/monoculture age and a maximum area of 10 ha. Within each area, 10 subsamples were randomly collected at 0–30 cm depth. In total, 1273 representative samples were obtained from alfalfa and oat pastures in Ayaviri and Macarí, Melgar Province (Figure 1), comprising 880 samples in Ayaviri and 393 in Macarí. The sampling network covered 84.16% of Ayaviri and 75.95% of Macarí, providing adequate spatial coverage to characterise soil variability within the study region.

2.3 | Soil Analysis

Soil samples were analysed at the Soil, Water, and Foliar Laboratories Network of the National Institute of Agricultural Innovation (LABSAF-INIA). Samples were pretreated, air-dried (< 40°C), and sieved to < 2 mm following ISO (2006). Analysed variables included texture (sand, silt and clay; NOM-021-RECNAT-2000 2002), pH (soil–water 1:1; EPA 2004), electrical conductivity (soil–water 1:5; ISO 1994); to convert EC measured in diluted soil–water extracts to the electrical conductivity of the saturated paste extract (ECe), we followed the procedure proposed by Kargas et al. (2022):

$$EC_e = \left(1.054 + \frac{283.4}{49.699 + 0.524 \times \text{Clay}\,\% - 0.339 \times \text{Sand}\,\%}\right) \times EC_{1:5}$$

Equivalent calcium carbonates (NOM-021-RECNAT-2000 2002), organic matter, organic carbon and total carbon (NOM-021-RECNAT-2000 2002). Available phosphorus was determined using method AS-11 for acidic to neutral soils (NOM-021-RECNAT-2000 2002). Exchangeable bases

TABLE 1 | Environmental predictor variables used for spatial modelling of the weighted Soil Quality Index (SQIw).

Variable group	Variable	Description
Topographic variables	Digital Elevation Model (DEM)	Elevation above sea level (derived from a DEM); used as a primary descriptor of topography and driver of soil formation and hydrology.
	Slope	Local gradient (degrees or %); controls runoff, erosion risk and soil depth distribution.
Topographic indices	Topographic Position Index (TPI)	Relative position of a cell within the landscape (ridge, valley, slope position); useful for mapping depositional/erosional zones.
	Terrain Ruggedness Index (TRI)	Metric of surface heterogeneity/roughness; related to soil redistribution processes.
	Topographic Wetness Index (TWI)	Proxy for spatial variation in soil moisture accumulation and saturation tendency (function of slope and upstream contributing area).

(Ca^{2+}, Mg^{2+}, K^+ and Na^+) were extracted with ammonium acetate, while exchangeable acidity and Al^{3+} were determined with potassium chloride (NOM-021-RECNAT-2000 2002). Effective cation exchange capacity (ECEC) was calculated as the sum of cations (Quispe et al. 2024). Bulk density (BD) and cation exchange capacity at pH 7 were obtained from SoilGrids (ISRIC-World Soil 2025) at 250 m resolution, averaging depths of 0–15 and 15–30 cm in QGIS. The exchangeable sodium percentage (ESP) is calculated as:

$$\mathrm{ESP} = \left(\frac{Na^+ \text{ exchangeable}}{\mathrm{ECEC}} \right) \times 100$$

where Na^+ and ECEC are expressed in cmolc kg^{-1}. This calculation allows soils to be classified according to functional sodicity in the context of international standards.

2.4 | Extraction and Processing of Geospatial Variables

Potential drivers of the spatial distribution of soil properties were compiled and selected as follows: landform (LF), derived from the geomorphological map at a scale of 1:250,000 (INGEMMET 2016); parent material (PM) and geological age (GA), from the national geological map at a scale of 1:100,000; soil type (ST), from SoilGrids with a 250 m resolution (ISRIC-World Soil 2025); life zone (LZ), at 1:100,000 (Aybar et al. 2017); and climate classification (CLI), at 1:400,000 (IDESEP 2020). These regionally scaled layers capture the principal environmental drivers—topography, lithology, pedology and climate—that govern the distribution of soil properties. Although the input datasets differ in thematic and positional accuracy, the selected resolutions are appropriate for detecting broad fertility patterns and for minimizing spatial inconsistencies.

For spatial prediction, the methodology employed environmental predictors that provide continuous spatial coverage across the study area, derived from remote sensing products and digital elevation models. The complete set of predictors and their sources are summarized in Table 1.

2.5 | Estimation of the Net Dispersive Clay Charge and the Gypsum Requirement

The net dispersive charge (NDC) was estimated as the difference between the dispersive charge (DC) and the flocculant charge (FC), both determined according to the effect of the ionicity of exchangeable cations (cmol kg^{-1}) on clay dispersion (Rengasamy et al. 2016).

$$\mathrm{DC} = (Ca) + 1.7(Mg) + 25(K) + 45(Na)$$

$$\mathrm{FC} = 45(Ca) + 27(Mg) + 1.8(K) + (Na)$$

$$\mathrm{NDC} = \mathrm{DC} - \mathrm{FC}$$

The agricultural gypsum requirement is normally calculated according to the amount of exchangeable sodium to be neutralised with Ca at a given depth (Oster et al. 2015).

$$\mathrm{GR} = 0.00086 \times \mathrm{BD} \times \mathrm{D} \times \mathrm{ECEC} \times (\mathrm{ESPi} - \mathrm{ESPf})$$

where ECEC (cmol kg^{-1}) is the effective cation exchange capacity obtained as the sum of exchangeable bases; BD ($g\,cm^{-3}$) is the soil bulk density; D (cm) is the sampling depth; ESP_i (%) is the current exchangeable sodium percentage of the soil; and ESP_f is the target value (5%) to be achieved with the application of agricultural gypsum. Finally, GR is the gypsum requirement expressed in $t\,ha^{-1}$.

2.6 | Exploratory Statistical Analyses for Variable Selection

Descriptive statistics (mean, variance, skewness, kurtosis, quartiles, etc.) were calculated for all variables, and normality was tested using the Shapiro–Wilk test. When necessary, data were transformed to approximate normal distributions. Pearson correlations ($p < 0.001$) were computed to identify variables related to plant health and detect multicollinearity. Principal component analysis (PCA) was then performed on standardized variables (*z*-scores) using the FactoMineR package, with visualization carried out using factoextra and ggplot2. Outputs included eigenvalues, variable contributions, $\cos^2$ values, and sample

TABLE 2 | Edaphological classification of saline and sodic soils and their main functional effects, according to pH, EC and ESP (Rengasamy 2010).

Class	Soil type	pH	EC_e ($dS\ m^{-1}$)	ESP (%)	Main characteristics
0	Non-salt-affected soil	6–8	<4	<6	Normal soil; limitations not related to salinity or sodicity
1	Acidic saline soil	<6	≥ 4	<6	Osmotic stress; toxicity of micronutrients (Fe, Al and Mn) and dominant anions
2	Neutral saline soil	6–8	≥ 4	<6	Osmotic stress dominant; possible toxicity of prevailing anion or cation
3	Alkaline saline soil	>8	≥ 4	<6	Osmotic stress; HCO_3^- and CO_3^{2-} toxicity; micronutrient toxicity at high pH
4	Acidic saline-sodic soil	<6	≥ 4	≥ 6	Osmotic stress; Na^+ toxicity; micronutrient toxicity
5	Neutral saline-sodic soil	6–8	≥ 4	≥ 6	Osmotic stress; Na^+ toxicity; dominant anion toxicity (Cl^- or SO_4^{2-})
6	Alkaline saline-sodic soil	>8	≥ 4	≥ 6	Osmotic stress; HCO_3^- and CO_3^{2-} toxicity; micronutrient toxicity at high pH
7	Acidic sodic soil	<6	<4	≥ 6	Indirect effects via soil structural degradation; seasonal waterlogging
8	Neutral sodic soil	6–8	<4	≥ 6	Structural problems; reduced infiltration; possible Na^+ toxicity
9	Alkaline sodic soil	>8	<4	≥ 6	Severe structural degradation; dispersion; HCO_3^- and CO_3^{2-} toxicity

distribution in factorial space. Biplots with confidence ellipses were generated to reveal latent structures. Although categorical variables were excluded from the PCA computation, the salinity–sodicity soil classification proposed by Rengasamy (2010) was used as a grouping variable to construct confidence ellipses in the space defined by the first two principal components, as described in Table 2.

2.7 | Development of a Soil-Quality Index for Saline and Sodic Soils (SQIw)

A soil quality index for saline–sodic soils (SQIw) was constructed using PCA-based multivariate weighting (Poma-Chamana et al. 2025). Twelve standardized indicators were analysed, with components explaining $\geq 60\%$ of variance retained. Variable contributions were combined into normalized weights, and indicators were rescaled to 0–1, inverting negatively associated ones (EC and ESP). Sensitivity was tested with alternative variance cutoffs (50%–80%).

2.8 | Comparative Analysis of SQIw Across Environmental and Soil Classes

Differences in SQIw across districts, textural classes, climate types and saline–sodic soil groups were assessed with non-parametric tests. A Kruskal–Wallis test identified overall effects ($p < 0.05$), followed by Dunn's pairwise comparisons with Bonferroni adjustment. Significant group differences were denoted with letters using multcompLetters from multcompView, and results were visualised with boxplots and jittered points in ggplot2 (Wickham 2016).

2.9 | Geostatistical Interpolation

The spatial variability of soil fertility supports optimised fertilisation through geostatistical modelling (Perez-Zapata et al. 2024). Using georeferenced soil analyses from Ayaviri and Macarí (BD, texture, pH, EC, OM, available P and K, CEC, exchangeable cations and lime requirement), Regression Kriging (RK) was applied for interpolation. Variogram analysis and RK modelling were conducted in SAGA v9.4 (Pásztor et al. 2016), and resulting maps were exported to QGIS v3.34 for spatial visualisation (Martínez 2020).

2.10 | Regression Kriging

Regression kriging is a hybrid technique in geospatial analysis that combines multiple linear regression with kriging to improve the prediction of spatial variables. A dependent variable is modelled against predictor variables, with kriging applied to the regression residuals. These predictor variables may be derived from remote sensing, digital elevation models, and other sources (Estrada-Godoy et al. 2023).

$$\hat{Z}(S_0) = \sum_{i=0}^{N} \lambda_i Z(S_i) \tag{5}$$

where $Z(S_i)$ tends towards the measure value at location i; S_i is an unknown estimate for the measured value at point i; N

corresponds to the measured values; and i denotes the prediction location (unidentified point) (Esri 2020).

2.11 | Model Validation

The nugget (C0), the sill (C0+C), the range (R) and the Sill-Nugget ratio (PSV) (Equation 6) are key parameters in semivariogram analysis, which describe the spatial autocorrelation of the data and are obtained from fitting the semivariogram model for geostatistical interpolation (Villatoro et al. 2008).

$$\mathrm{PSV} = \frac{\mathrm{Sill} - \mathrm{Nugget}}{\mathrm{Sill}} = \frac{\mathrm{C}}{\mathrm{C}_0 + \mathrm{C}} \tag{6}$$

The selection of the semivariogram model is based on criteria such as the root mean square error (RMSE), the coefficient of determination (R^2), and the mean absolute error (MAE) (Bromberg and Pérez 2012). The optimal model should yield RMSE (Equation 7) and MAE (Equation 8) values close to zero, and R^2 (Equation 9) values close to one, as these indicate the accuracy and quality of the model, respectively (Fu et al. 2024). Kriging interpolations for each soil property were cross-validated using the leave-one-out method (Fernández Villafañez 2022).

$$\mathrm{RMSE} = \sqrt{\frac{1}{n}\sum_{i=1}^{n}\left[Z_1(x_i) - Z_2(x_i)\right]^2} \tag{7}$$

$$\mathrm{MAE} = \frac{1}{n}\sum_{l=1}^{n}\left|Z_1(x_i) - Z_2(x_i)\right| \tag{8}$$

$$R^2 = 1 - \frac{\sum_{i=1}^{n}\left[Z_1(x_i) - Z_2(x_i)\right]^2}{\sum_{i=1}^{n}\left[Z_1(x_i) - Z_1\right]^2} \tag{9}$$

where n represents the number of samples, $Z_1(x_i)$ y $Z_2(x_i)$ denote the predicted and observed at site i, respectively.

3 | Results

3.1 | Descriptive Statistics of the Physicochemical Properties of Soils in Ayaviri and Macarí

Descriptive statistics of 29 edaphoclimatic variables derived from 1273 soil samples are summarized in Table 3. Soil pH exhibited a wide range, from strongly acidic to alkaline conditions (4.50–9.70), with most values concentrated between slightly acidic and neutral ranges (interquartile range: 5.50–6.60). Electrical conductivity also showed marked variability (0.10–35.76 dS m^{-1}), indicating the coexistence of non-saline and highly saline soils within the study area. Calcium carbonation content ranged from 0% to 42.60%, reflecting heterogeneous degrees of carbonatation, while organic matter varied between 0.50% and 12.10%, consistent with contrasting land use and management conditions, consistent with predominantly loam textures.

Cation base analysis revealed flocculant charge (822.8 cmol kg^{-1}) exceeded dispersive charge (197.7 cmol kg^{-1}), yielding a negative net dispersive charge (−625.2 cmol kg^{-1}), though some soils showed severe dispersion (max. 654.1). The exchangeable sodium percentage (ESP) ranged from 0.12% to 86.76%, with a substantial proportion of samples exceeding commonly accepted sodicity thresholds. This wide ESP range, together with low Ca^{2+} and Mg^{2+} contents and reduced ECEC in several soils, indicates the presence of sodicity risk even under acidic to near-neutral pH conditions, highlighting the occurrence of acid–sodic and saline–sodic soil environments.

Bulk density was homogeneous ($1.27 \pm 0.08\,\mathrm{g\,cm^{-3}}$), gypsum requirement was highly variable (0–82.7 t ha^{-1}, mean 8.30 ± 5.45), and both mean temperature (8.55°C) and MSAVI (0.58 ± 0.14) followed near-normal distributions. Overall, these statistics demonstrate marked edaphoclimatic heterogeneity, justifying multivariate analyses to identify and weight key drivers of sodic soil quality.

3.2 | Pearson Correlations Between Gypsum Requirement (GR), Salt-Affected Soil Properties and Environmental Covariates in the Districts of Ayaviri and Macarí, Puno

Pearson correlation analysis ($p < 0.001$) revealed significant associations between ESP, NDC, GR, and edaphoclimatic variables in soils from Macarí and Ayaviri (Figure 2). ESP correlated positively with NDC (0.53) and GR (0.52), but negatively with FC (−0.52), ECEC (−0.52), Ca^{2+} (−0.51) and Mg^{2+} (−0.43). NDC showed strong negative correlations with FC (−1.00), Ca^{2+} (−1.00) and ECEC (−0.99). GR was positively related to Na (0.87), DC (0.66) and ESP (0.52), but negatively to FC (−0.31) and Ca^{2+} (−0.31), indicating that higher sodicity and dispersion increase gypsum requirements, while flocculation and calcium mitigate them.

For PCA and SQI development (Figure 2), 10 representative variables covering chemical (pH, OM, ESP and CM), physical (clay percentage and bulk density), structural (DC and FC), climatic (Tmean) and biological (MSAVI) dimensions were selected, excluding highly collinear pairs ($|r| > 0.80$). This approach captured key variability of sodic soils, linking structural stability, vegetation response and environmental conditions to a robust soil quality index.

3.3 | Edaphic Gradients Associated With the Soil Quality Index (SQIw) Revealed Through Principal Component Analysis

The SQIw was derived from a subset of non-collinear edaphic indicators, selected for their mechanistic relevance to soil acidity, salinity and sodicity processes. The variables considered comprised exchangeable sodium percentage (ESP), exchangeable Na^+, the Ca^{2+}/Mg^{2+} ratio, electrical conductivity (EC), dispersive and flocculant clay charges (DC, FC), organic matter (OM), mean annual temperature (Tmean) and the Modified Soil-Adjusted Vegetation Index (MSAVI). Collectively, these indicators enable the SQIw to synthesize sodicity severity, structural stability and the functional response of the soil–plant system. To examine fertility gradients

TABLE 3 | Descriptive statistics of 28 physicochemical variables and the agricultural gypsum requirement of soils from the Ayaviri and Macari districts, Puno.

Variable	Units	Mean	SD	Var	CV	Skewness	Kurtosis	Min	Max	P25	Median	P75
pH	Ratio	6.15	0.90	0.82	14.71	0.80	0.28	4.50	9.70	5.50	6.00	6.60
ECe	$dS\ m^{-1}$	3.28	4.65	21.60	141.67	3.50	12.96	0.10	35.76	0.98	2.27	3.14
$CaCO_3$	%	2.05	4.98	24.79	242.33	3.35	12.46	0.00	42.60	0.00	0.00	1.70
OM	%	4.03	2.13	4.55	52.91	0.68	−0.06	0.50	12.10	2.30	3.60	5.40
Pav	$mg\ kg^{-1}$	31.99	59.15	3498.97	184.89	5.28	39.92	0.10	719.90	7.40	14.30	28.60
Kav	$mg\ kg^{-1}$	282.62	344.28	118531.50	121.82	7.50	91.38	3.10	6140.00	124.00	195.50	312.80
Sand	%	37.09	11.79	138.95	31.79	−0.01	−0.45	0.39	71.38	28.53	37.03	45.89
Clay	%	18.68	7.47	55.81	39.99	1.05	1.95	3.47	60.48	13.32	17.68	22.70
Silt	%	44.23	9.97	99.46	22.55	0.34	0.59	13.61	80.73	37.21	43.93	50.22
Ca^{+2}	$cmol\ kg^{-1}$	17.03	28.15	792.17	165.29	4.27	19.53	0.70	201.00	4.70	9.60	17.00
Mg^{+2}	$cmol\ kg^{-1}$	1.91	1.82	3.31	95.06	3.08	14.53	0.20	17.96	0.80	1.40	2.30
Na^{+}	$cmol\ kg^{-1}$	3.54	1.73	2.98	48.82	4.93	47.45	0.10	27.75	3.11	3.40	3.71
K^{+}	$cmol\ kg^{-1}$	0.73	0.89	0.79	122.22	7.37	87.62	0.10	15.70	0.31	0.50	0.80
Al^{+3}	$cmol\ kg^{-1}$	0.06	0.28	0.08	470.07	8.29	92.31	0.00	4.70	0.00	0.00	0.00
H^{+}	$cmol\ kg^{-1}$	0.19	0.60	0.36	323.44	10.28	153.37	0.00	11.70	0.00	0.00	0.10
DC	$cmol\ kg^{-1}$	197.65	88.36	7808.24	44.71	3.91	31.22	13.14	1320.89	164.74	182.30	210.41
FC	$cmol\ kg^{-1}$	822.82	1281.51	1642255.00	155.74	4.18	18.89	43.80	9102.86	245.69	492.64	827.20
NDC	$cmol\ kg^{-1}$	−625.17	1247.91	1557290.00	−199.61	−4.24	19.28	−8735.96	654.11	−627.10	−297.16	−76.74
ECEC	$cmol\ kg^{-1}$	23.45	28.84	831.75	122.97	4.05	17.91	4.65	206.70	9.90	15.98	24.20
ECP	%	58.84	18.98	360.35	32.26	−0.30	−0.44	4.12	99.26	45.85	61.01	72.05
EMP	%	9.89	6.63	43.98	67.03	2.96	16.36	0.29	73.49	5.91	8.42	11.85
ESP	%	23.90	13.90	193.08	58.15	0.60	−0.16	0.12	86.76	13.80	21.15	32.51
EPP	%	5.04	5.70	32.45	113.05	4.11	29.12	0.06	68.92	1.75	3.32	6.36
EAP	%	0.70	2.52	6.36	357.95	6.97	59.81	0.00	32.50	0.00	0.00	0.33
$(Ca^{+2}+Mg^{+2})/K^{+}$	Ratio	46.63	104.76	10973.92	224.64	7.16	66.50	0.25	1574.00	8.80	20.33	44.50
Ca^{+2}/Mg^{+2}	Ratio	9.96	17.91	320.68	179.72	10.59	156.66	0.06	331.39	4.13	6.57	9.95

(Continues)

TABLE 3 | (Continued)

Variable	Units	Mean	SD	Var	CV	Skewness	Kurtosis	Min	Max	P25	Median	P75
Mg^{+2}/K^{+}	Ratio	4.18	4.62	21.31	110.33	3.05	14.72	0.09	47.00	1.24	2.69	5.33
BD	$g\,cm^{-3}$	1.27	0.08	0.01	6.05	−14.18	231.00	0.00	1.34	1.26	1.28	1.30
GR	$t\,ha^{-1}$	8.30	5.45	29.73	65.72	4.48	43.27	0.00	82.72	6.47	8.55	9.85

associated with the SQIw and their relationship with gypsum requirement (GR), a principal component analysis (PCA) was subsequently performed, with sample distributions interpreted against chemical classes of saline and sodic soils as defined by Rengasamy (2010).

The PCA identified two main components explaining 46.04% of the total variance (Figure 3). The first principal component (PC1; 27.60%) represented a structural stability–salinity gradient, contrasting soils characterized by high flocculant charge (contribution: 21.96%) and greater structural stability with soils exhibiting elevated sodicity (ESP: 14.80%) and dispersive charge (5.26%), which are associated with reduced porosity and aggregate stability. Electrical conductivity (EC; 13.18%) and the Ca/Mg ratio (12.20%) further reinforced the influence of salinity and cation balance on this gradient. The second principal component (PC2; 18.44%) captured variability related to sodicity mitigation and soil physical condition. Gypsum requirement (22.98%) reflected the intensity of amendment demand, while dispersive charge (18.68%) highlighted clay instability under limited Ca^{2+} availability. Organic matter (9.29%) contributed positively through organo–mineral interactions that enhance aggregation, whereas bulk density (4.08%) reflected compaction effects on aeration and hydraulic properties. Mean temperature (15.65%) further modulated these processes by influencing organic matter turnover and amendment efficiency.

Taken together, PC1 and PC2 describe complementary edaphic gradients: PC1 reflects trade-offs between structural stability and salinity–sodicity stress, whereas PC2 integrates amendment requirements, organic matter, and climatic effects regulating sodicity dynamics. These results underscore the usefulness of the SQIw as a synthetic indicator integrating sodicity, structural stability and porosity for assessing soil health under heterogeneous acid–sodic and saline–sodic conditions.

3.4 | A Non-Parametric Assessment of the Weighted Soil Quality Index (SQIw) Among Districts, Soil Textural Classes, Salinity–Sodicity Classifications and Climate Types

Significant differences in SQIw were observed across districts, soil textures, salinity–sodicity classes, and climate types (Figure 4). Soils in Macarí (0.61) had higher SQIw than those in Ayaviri (0.44; p.adj < 0.001), mainly due to lower gypsum requirements and bulk density, which favoured Ca^{2+} accessibility and structural recovery. Regarding texture, clay-rich soils (e.g., Clay, Silty Clay Loam and Clay Loam) showed higher SQIw than Sandy Loam (0.36; p.adj ≤ 0.01), reflecting the stabilizing role of clay content. By salinity–sodicity type, acid–saline–sodic (0.38) and acid–sodic soils (0.40) had significantly lower SQIw than neutral and alkaline categories (p.adj < 0.01), confirming the penalizing effect of combined acidity and sodicity. Finally, under SENAMHI climate classes, soils in B(o,i)C′ (cold–humid, 0.61) outperformed those in C(o,i)C′ (cold–semiarid, 0.46; p.adj < 0.0001), as higher water availability and OM stabilization enhanced aggregate formation, effective CEC, and resilience to sodicity.

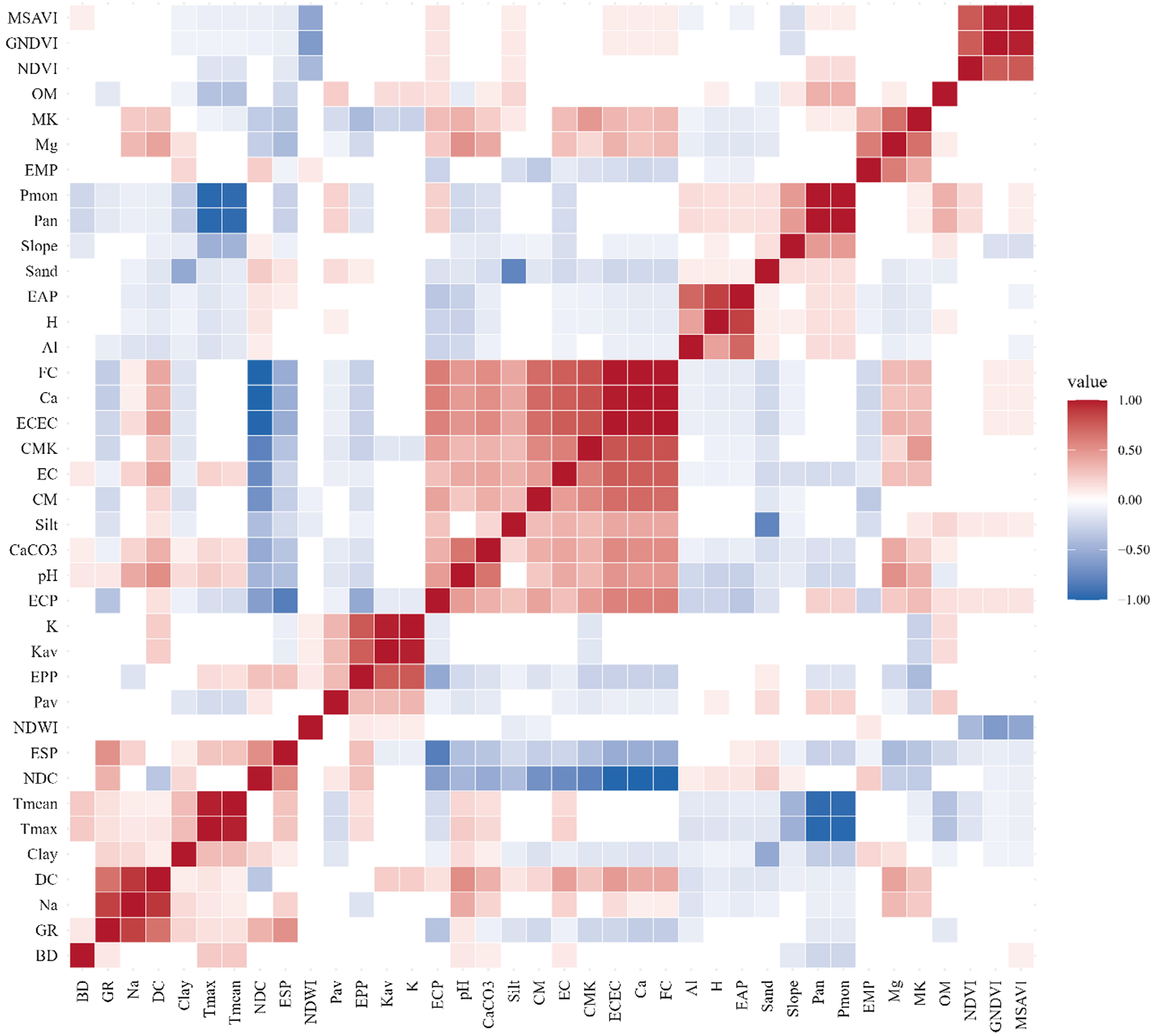

FIGURE 2 | Pearson correlation matrix of bivariate parametric correlations between Gypsum Requirement (GR) and 28 soil physicochemical variables, complemented with climatic variables and vegetation spectral indices. Only statistically significant correlations ($p < 0.001$) are presented. CMK = $(Ca^{2+} + Mg^{2+})/K^{+}$; CM = Ca^{2+}/Mg^{2+}; MK = Mg^{2+}/K^{+}; ESP, EPP, ECP, BD, bulk density; EMP, exchangeable sodium, potassium, calcium and magnesium percentages; ECEC, effective cation exchange capacity.

3.5 | Spatial Variation of Soil Sodicity and Agricultural Gypsum Requirement in the Districts of Ayaviri and Macarí

Pearson correlations combined with PCA enabled the refinement of predictors for gypsum requirement (GR), selecting ESP, FC, Na^{+} and MSAVI as the most representative edaphic and spectral variables (Figures 5 and 6). Semivariogram analysis (Table 4) indicated that the exponential model best described GR variability, with moderate spatial dependence in Ayaviri (PSV = 0.49) and strong dependence in Macarí (PSV = 0.23). Autocorrelation ranges exceeding 19 km confirmed a regional-scale spatial structure.

Model performance was evaluated using complementary statistical indicators (Table 4). The coefficient of determination (R^2) quantified the proportion of GR variability explained by the model, indicating high explanatory power in both districts (0.97 in Ayaviri and 0.85 in Macarí). RMSE assessed the magnitude of prediction errors and its sensitivity to large deviations, while MAE represented the average absolute error, providing a more robust measure less influenced by extreme values. The combined use of these indicators allows a comprehensive evaluation of predictive accuracy and model reliability. The low RMSE (1.01 and 1.74 $t\,ha^{-1}$) and MAE (0.41 and 1.06 $t\,ha^{-1}$) values confirm the robustness of the Regression Kriging approach. Consequently, the generated GR maps constitute reliable tools

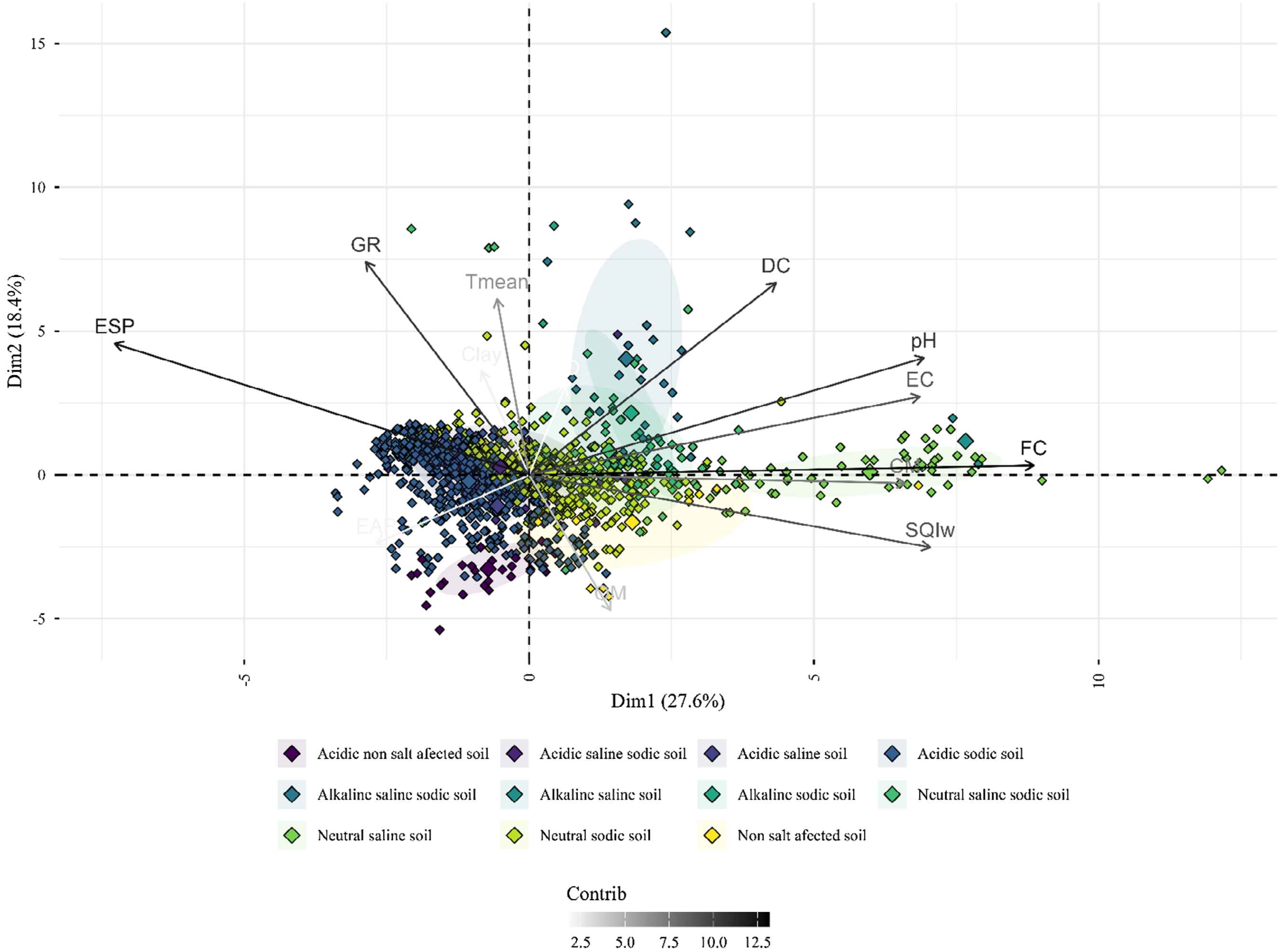

FIGURE 3 | Principal Component Analysis [PCA] of edaphic variables: Multivariate distribution across different saline and sodic soil classes on axes Dim1 (27.6%) and Dim4 (18.4%), with 44% confidence ellipses.

for guiding amendment planning and site-specific sodicity management.

Regression Kriging maps (Table 5; Figure 7) revealed marked spatial contrasts between districts. In Ayaviri (85,580.2 ha), 59.6% of land required $\leq$9.53 t ha^{-1} gypsum, while 40.4% exceeded this threshold, indicating substantial high-dose demand. In contrast, in Macarí (52,506.2 ha), most land required moderate to low doses ($\leq$9.6 t ha^{-1} in 92.2% of the area). These patterns support differentiated zoning: in Ayaviri, large-scale interventions should focus on central and southern lowlands with high ESP and low FC (≈2756 ha of priority land), whereas in Macarí, localized applications in the southeast and northwest are more cost-effective and reduce the risk of over-application.

4 | Discussion

4.1 | Development and Validation of the Weighted Soil Quality Index (SQIw)

The construction of a Soil Quality Index oriented towards sodicity (SQIw) represents a significant methodological contribution. Unlike generic soil quality indices (Doran and Parkin 2015), the SQIw developed in this study is specific to acid–saline–sodic soils, integrating chemical variables (ESP, pH and ECEC), physical variables (BD, % clay), structural variables (DC and FC), and climatic variables (Tmean), selected through correlation analysis and multicollinearity control.

Principal component analysis (PCA) revealed that PC1 and PC2 together explained 46.04% of the total variance, delineating two key functional gradients: (i) structural stability and salinity (PC1), and (ii) the interaction between texture, organic matter, and climatic conditions (PC2). This duality reflects the complexity of sodic soils, where recovery depends not only on cation exchange processes but also on factors such as porosity, temperature and the availability of organic binding agents.

The systematic reduction in SQIw observed in acid–saline–sodic soils (median = 0.38), relative to neutral or alkaline soils (0.61–0.74), indicates a pronounced negative synergy between acidity and sodicity that constrains the vegetative development of cultivated pasture. Moreover, in the soils analysed, Ca saturation was markedly lower (mean = 58.84 ± 18.98%; median = 45.85%), which diminishes clay flocculation and aggregate stability (Quispe et al. 2024). Under these conditions, even low amounts of exchangeable Na (6%) can provoke substantial clay dispersion in acidic soils, owing to the substantially greater dispersive potency of Na relative to Ca (Rengasamy 2002, 2010).

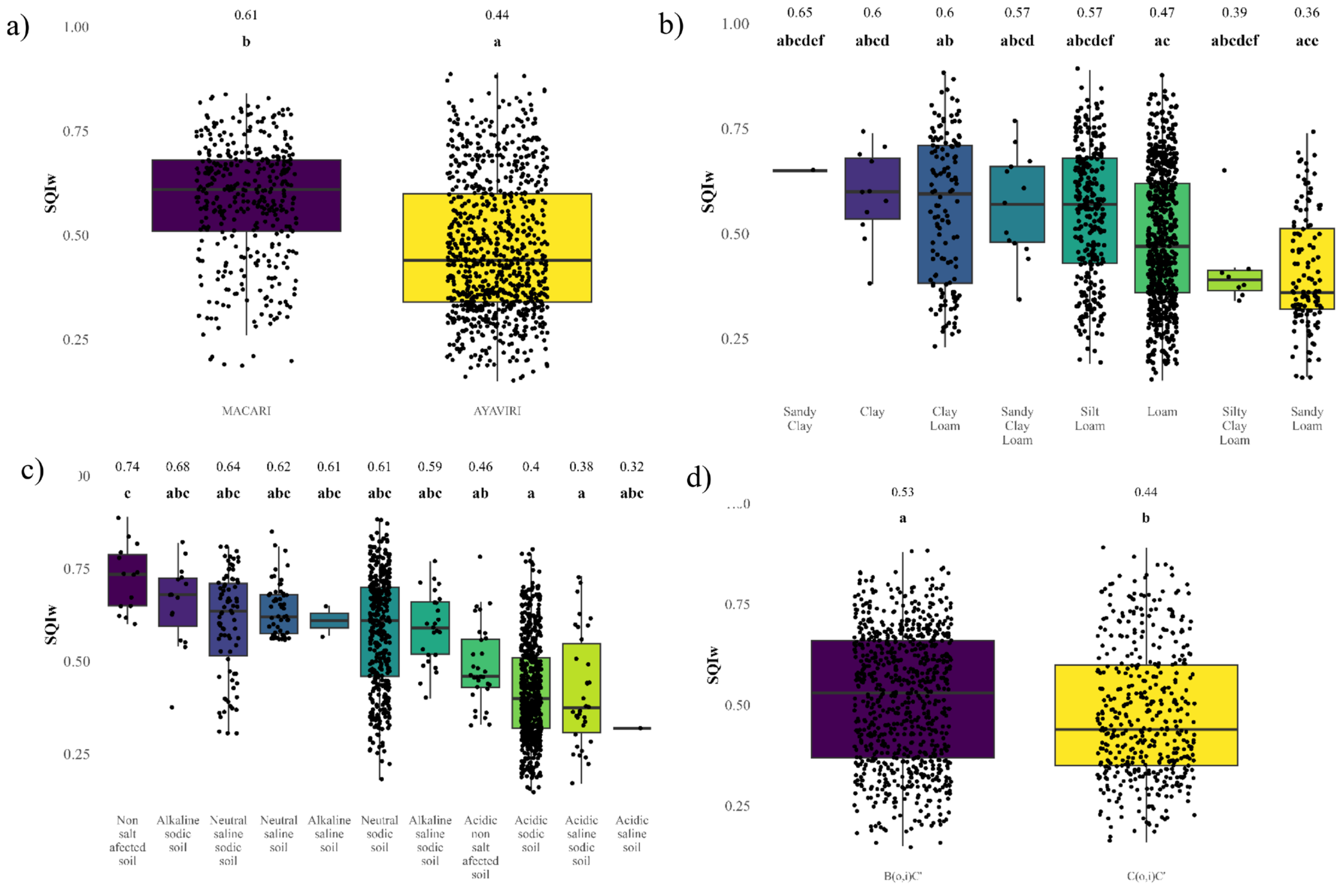

FIGURE 4 | Weighted Soil Quality Index (SQIw) according to different factors. (a) Comparison of SQIw between the districts of Ayaviri and Macarí; (b) comparison of SQIw among different soil textural classes; (c) comparison of SQIw among saline and sodic soil types; and (d) comparison of SQIw among climate types. Dunn's post hoc test following Kruskal–Wallis, with Bonferroni correction for multiple comparisons, was applied. Different letters denote statistically significant differences.

This phenomenon is exacerbated by low pH, which reduces the efficacy of flocculating cations and promotes structural instability, as widely documented for acidic sodic soils (Rengasamy et al. 2016; Bello et al. 2021; Noonari et al. 2025). In addition, acidity restricts microbial activity and the decomposition of soil organic matter, thereby limiting the formation of stable aggregates (Vista et al. 2024; Mitsuta et al. 2025).

The inclusion of the Modified Soil-Adjusted Vegetation Index (MSAVI) as a biological indicator within the SQIw reinforces its validity, since MSAVI is sensitive to vegetation cover in areas with high background reflectance, such as High-Andean pastures. The negative correlation between GR and MSAVI (Figure 2) suggests that soils with higher gypsum requirements exhibit lower vegetation vigour, thereby supporting the use of the SQIw as a diagnostic tool for ecosystem health. Nevertheless, the SQIw requires supervision through calibrations or crop monitoring to ensure that it continues to reflect changes under different agricultural conditions (Ozlu et al. 2022).

4.2 | Edaphoclimatic Controls on Sodicity and Gypsum Requirement

The zoning analysis revealed marked differences between Ayaviri and Macarí in both sodicity risk intensity and the areal extent of agricultural land affected. Soils in Ayaviri exhibited significantly lower SQIw values (median = 0.44) than those in Macarí (0.61), principally attributable to higher gypsum requirement (GR), greater bulk density (BD) and elevated exchangeable sodium percentage (ESP). This increased level of degradation is likely associated with poor drainage, intensive irrigation practices that promote upward Na^+ flux via surface evaporation, and potentially reduced inputs of organic matter (Stavi et al. 2021).

From a textural standpoint, sandy loam soils (median SQIw = 0.36) were the most vulnerable, whereas loam and clay-loam soils demonstrated greater resilience. Higher clay contents (13.3%–22.7%) foster aggregate stability and enhanced cation-exchange capacity (CEC), thereby mitigating Na-induced colloidal dispersion (Bi et al. 2023; Niaz et al. 2023). Classification by salinity and sodicity further confirmed that acid–saline–sodic soils represent the most advanced state of degradation, underscoring the need for integrated management strategies that simultaneously address sodicity, acidity (via liming) and salinity (via leaching) (Daba 2025).

The mean GR (8.30 $t\,ha^{-1}$), with maxima reaching 82.72 $t\,ha^{-1}$, may appear paradoxical in soils with an average pH of 6.15, given that high gypsum requirements are conventionally associated with alkaline soils. However, in acid–sodic soils elevated GR values arise from the concurrence of several processes: (i)

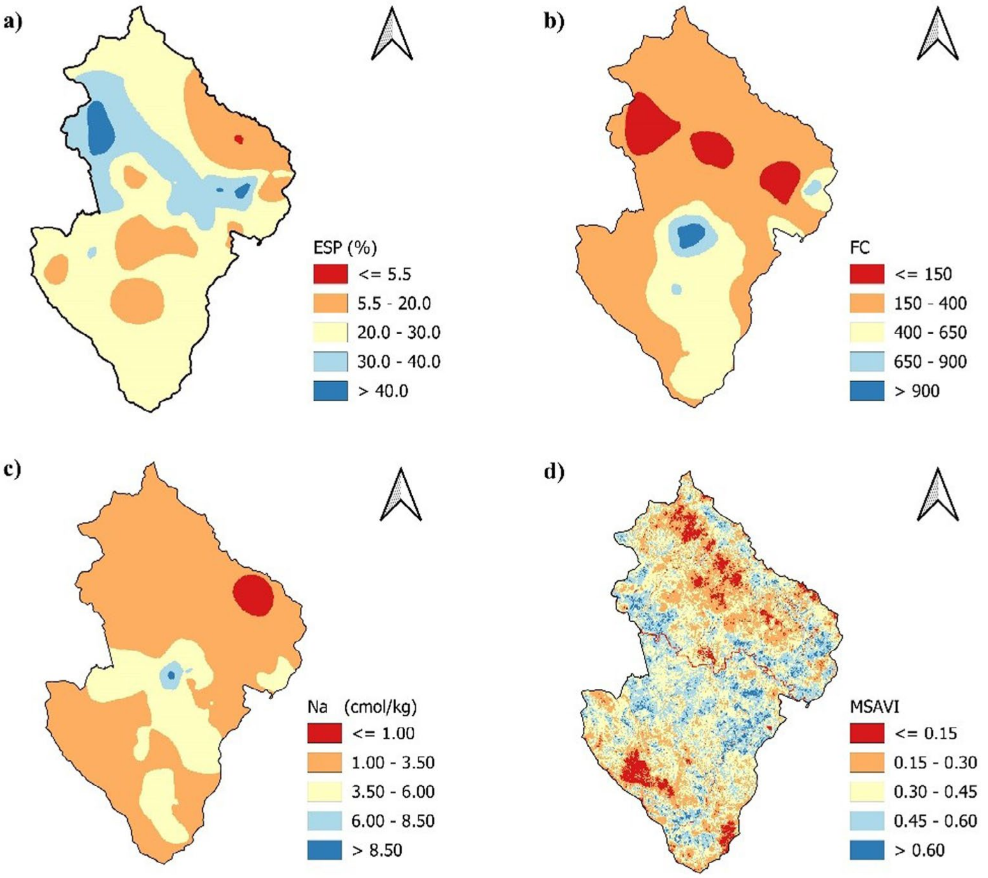

FIGURE 5 | Spatial maps of vegetation and soil predictor variables in the Ayaviri district: (a) Exchangeable sodium percentage, (b) Flocculant charge, (c) Exchangeable sodium concentration and (d) Soil-adjusted vegetation index.

high ESP (23.9%), which necessitates substantial Ca^{2+} inputs to displace Na^+ from the exchange complex; (ii) reduced gypsum efficacy under acidic conditions owing to interactions of Ca^{2+} with Al^{3+} and acidic fractions of organic matter; and (iii) diminished hydraulic conductivity driven by dispersion, which limits Na^+ leaching (Ahmad et al. 2016). Collectively, these mechanisms render the remediation of acid–sodic soils more input-intensive than that of alkali–sodic counterparts (Bello et al. 2021; Daba 2025).

A limitation of the present study is the absence of soluble anion analyses, which constrains a full appraisal of ionic balance and potential Ca precipitation processes. Nevertheless, the occurrence of soils with pH < 5.5 and ESP > 30% suggests that sodicity within the Peruvian Altiplano is predominantly driven by Na^+ inputs from saline groundwater—potentially associated with Ayaviri River tributaries—combined with acidic parent materials that limit base saturation. Comparable conditions have been documented in volcanic terrains of Ethiopia and Indonesia, where sodicity develops under acidic regimes with strong hydrogeological control, emphasizing the need for diagnostic frameworks tailored to acid–sodic environments.

Gypsum effectiveness is additionally conditioned by soil structural and biological factors such as porosity, organic-matter content and the prevailing leaching regime. Combined applications of gypsum and organic amendments have been shown to improve flocculation, aggregate stability and soil biological activity (Niaz et al. 2022; Tian et al. 2024). While this strategy is well established for alkali soils (Singh et al. 2023), it may confer even greater benefits under acidic conditions.

Finally, the C(o,i)C′ (cold–semi-arid) climatic class exhibited lower SQIw values than the B(o,i)C′ (cold–humid) class, indicating that moisture deficits constrain natural leaching of salts and the stabilization of organic matter, thereby exacerbating degradation processes (Shi 2022). Although shallow groundwater, microdepressions and textural variability appear to account for much of the spatial distribution of sodicity, these hypotheses warrant validation through direct groundwater level measurements or local hydrological modelling. Based on the zoning results, priority intervention areas include the central and southern lowlands of Ayaviri and the south-eastern and north-western sectors of Macarí, where gypsum requirements exceed 9.6 $t\,ha^{-1}$.

4.3 | Spatial Prediction of Agricultural Gypsum Requirement

There is strong evidence of synergy when applying regression kriging in combination with edaphic and vegetation covariates for the spatial prediction of gypsum requirement (GR) in the reclamation of sodic soils (Jalane et al. 2024). This approach achieved high predictive performance, with coefficients of determination (R^2) of 0.97 in Ayaviri and 0.85 in Macarí, and mean

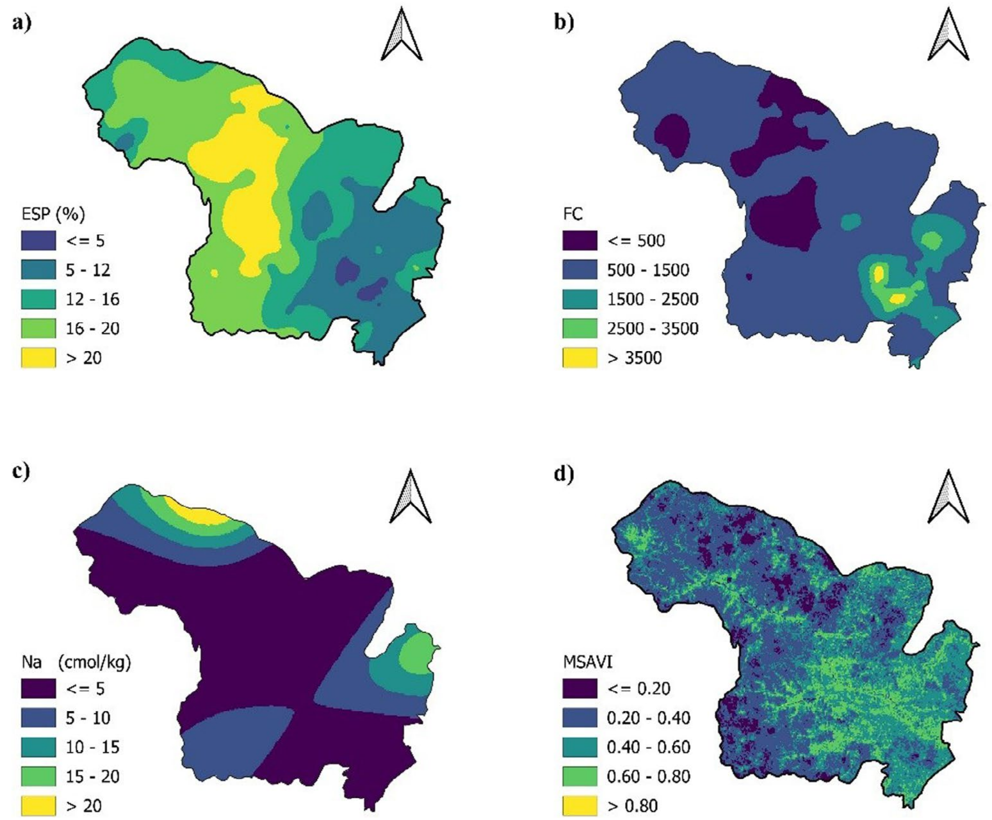

FIGURE 6 | Spatial maps of vegetation and soil predictor variables in the Macarí district: (a) Exchangeable sodium percentage, (b) Flocculant charge, (c) Exchangeable sodium concentration and (d) Soil-adjusted vegetation index.

TABLE 4 | Semivariogram models of soil liming requirement in the districts of Macarí and Ayaviri.

		Nugget	Sill	Range	PSV	Cross validation		
District	**Model**	C_0	C_0+C	m	C/C_0+C	R^{2}[a]	RMSE[b]	MAE[c]
Ayaviri	Exponential	12.02	23.41	24446.05	0.49	0.97	1.01	0.41
Macari	Exponential	11.43	14.81	19839.02	0.23	0.85	1.74	1.06

[a]Coefficient of determination.
[b]Root-mean-square error.
[c]Mean absolute error.

absolute errors (MAE) consistently below 1.1 t ha^{-1}. Such accuracy clearly exceeds that reported in previous studies on gypsum application and sodic soil management (Gashi et al. 2025; Green et al. 2023), reinforcing the reliability of the predictive models for soil management in the Peruvian Altiplano.

The GR maps generated through regression kriging constitute a high-value operational tool for extension services, farmers, and decision-makers. In Ayaviri, 95.77% of the agricultural area requires between 9.53 and 19.05 t ha^{-1} of gypsum, implying substantial input demand and application logistics. In Macarí, 78.90% of the area requires between 5.6 and 9.6 t ha^{-1}, indicating a less critical but still significant scenario. These rates are comparable to those reported in sodic regions of the United States, India, and Australia, where GR typically ranges from 5 to 25 t ha^{-1} (Morsy et al. 2022; Oster et al. 2015).

In addition, the availability and cost of agricultural gypsum in the region must be considered. In the absence of local sources, transportation may render large-scale amendment economically unfeasible. Therefore, alternative calcium sources, such as steel slag or construction gypsum, should be explored, provided their agronomic effectiveness and environmental safety are properly evaluated.

This study addresses a critical yet underexplored issue in High-Andean agroecosystems: the spatial variability of sodicity and its implications for calcium amendment requirements, specifically agricultural gypsum ($CaSO_4 \cdot 2H_2O$). By integrating multivariate analysis, advanced geostatistics (regression kriging) and GIS tools, we achieved highly accurate modelling of the spatial distribution of GR, providing a solid technical basis for site-specific management in forage systems.

Regression kriging (RK) models demonstrated exceptional predictive capacity, with coefficients of determination (R^2) of 0.97 in Ayaviri and 0.85 in Macarí, and MAE values below 1.1 t ha^{-1}. These values substantially exceed the accuracy standards recommended for digital soil mapping studies (Hengl et al. 2017; Odeha et al. 1994), validating the robustness of the models and their applicability in agronomic decision-making. The high predictive performance is largely attributable to the selection of optimal covariates (ESP, flocculant charge, exchangeable Na^+ and MSAVI), which capture both key soil processes and vegetation responses, thereby reducing the uncertainty inherent in spatial interpolation.

TABLE 5 | Zones of agricultural gypsum requirement in soils of the districts of Ayaviri and Macarí.

District	GR class ($t\,ha^{-1}$)	Agricultural area (ha)	Percentage of total agricultural area (%)
Ayaviri	< 9.53	50976.45	59.57
	9.53–19.05	31847.76	37.21
	19.05–28.58	1989.07	2.32
	28.58–38.11	619.09	0.72
	> 38.11	147.83	0.17
	Total affected area	85580.20	100
Macarí	< 9.53	769.08	1.46
	9.53–19.05	6199.22	11.81
	19.05–28.58	26428.31	50.33
	28.58–38.11	14998.84	28.57
	> 38.11	4110.77	7.83
	Total affected area	52506.22	100

Moderate spatial dependence in Ayaviri (PSV = 0.49) and strong dependence in Macarí (PSV = 0.23) reflect differences in edaphic heterogeneity between districts, possibly linked to geological, hydrological and land-use factors. The large autocorrelation ranges (19–24 km) indicate that sodicity processes are not localized but operate at a regional scale, justifying watershed- or district-level management interventions. This finding is consistent with studies in arid and semi-arid regions where sodicity exhibits spatial patterns structured by drainage, texture and irrigation water use (Mohanavelu et al. 2021; Shahid et al. 2018).

These results contrast with traditional approaches that apply uniform gypsum rates without considering spatial variability, leading to risks of overdosing (economic and environmental inefficiency) or underdosing (insufficient reclamation). This study demonstrates that site-specific management is not only feasible but necessary in heterogeneous landscapes such as the Peruvian Altiplano, where small variations in topography, texture or hydrological regime can generate large differences in soil condition.

From a methodological perspective, the high predictive performance achieved through regression kriging ($R^2 = 0.97$ in Ayaviri; $R^2 = 0.85$ in Macarí) and the observed autocorrelation ranges (~19–24 km) validate the usefulness of combining edaphic and vegetation covariates to map gypsum requirements at the district scale. These results support the applicability of digital approaches (RK + GIS) in mountainous regions, where separating deterministic and spatial components facilitates mapping in complex terrain (De Caires et al. 2025). Nevertheless, the practical robustness of the maps critically depends on sampling density and covariate representativeness, as highlighted by Dash et al. (2024). Therefore, uncertainty analysis and spatial validation are recommended prior to large-scale implementation.

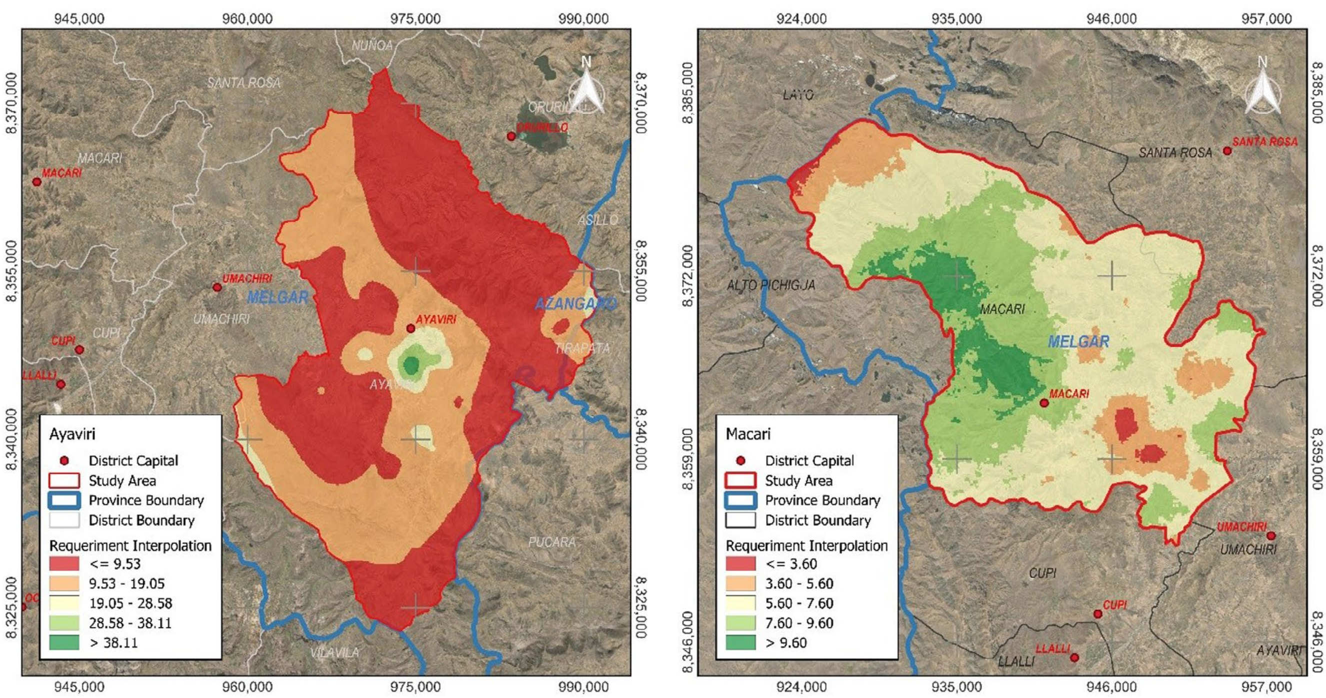

FIGURE 7 | Agricultural gypsum requirement ($t\,ha^{-1}$) of soils in the districts of (a) Ayaviri and (b) Macarí.

4.4 | Limitations

The present assessment is based predominantly on surface samples (0–30 cm) and on indirect hydrological indicators; subsequent work should therefore incorporate deeper soil profiles, groundwater-table depth and irrigation-water quality to elucidate mechanisms of sodium accumulation and transport in acid soils. Equally, the routine omission of anion analyses (Cl^-, SO_4^{2-}, HCO_3^-) from standard diagnostic protocols limits characterization of ionic equilibria and reduces the capacity to predict soil responses to calcium-based amendments. The limited availability of local gypsum sources further emphasizes the need to evaluate alternative calcium-rich materials and to assess their agronomic efficacy and logistical feasibility. Finally, field-scale validation trials are required to quantify crop and pasture responses to spatially differentiated gypsum rates and to determine the outcomes of combined amendment strategies (gypsum, liming and organic matter additions) under prevailing acid–sodic conditions.

5 | Conclusions

This study developed an integrated framework for assessing soil sodicity and agricultural gypsum requirement in High-Andean forage systems through the combination of soil quality indicators, geostatistical modelling and spatial analysis. The proposed Sodicity-oriented Soil Quality Index (SQIw), based on structural, chemical, physical and climatic variables, proved useful for identifying vulnerable soils and supporting the spatial diagnosis of sodicity-related processes.

The application of regression–kriging and spatial modelling highlighted the importance of considering the spatial variability of sodicity when planning gypsum application strategies. The resulting maps provide a basis for identifying priority intervention areas and improving site-specific soil management in High-Andean environments.

From a management and policy perspective, the SQIw and spatially explicit GR outputs provide practical decision-support tools for prioritising interventions, improving gypsum application strategies and supporting sustainable soil management in High-Andean agroecosystems. The methodological framework presented is transferable to other Andean catchments and comparable mountain agroecosystems and can inform the design of local policy instruments that respond to increasing climatic variability and land-use pressure.

Overall, the findings underscore the relevance of integrating soil quality indices with spatially explicit modelling frameworks to enhance the diagnosis of sodicity processes and optimise gypsum requirement estimation in vulnerable High-Andean agroecosystems.

Funding

This research was funded by the INIA project CUI 2487112 'Mejoramiento de los servicios de investigación y transferencia tecnológica en el manejo y recuperación de suelos agrícolas degradados y aguas para riego en la pequeña y mediana agricultura en los departamentos de Lima, Áncash, San Martín, Cajamarca, Lambayeque, Junín, Ayacucho, Arequipa, Puno y Ucayali'.

Conflicts of Interest

The authors declare no conflicts of interest.

Data Availability Statement

The data that support the findings of this study are available from the corresponding author upon reasonable request.

References

Ahmad, S., A. Ghafoor, M. E. Akhtar, and M. Z. Khan. 2016. "Implication of Gypsum Rates to Optimize Hydraulic Conductivity for Variable-Texture Saline–Sodic Soils Reclamation." *Land Degradation & Development* 27, no. 3: 550–560. https://doi.org/10.1002/ldr.2413.

Anderson, A. W., U. Gull, S. E. Benes, et al. 2023. "Salinity and Cultivar Effects on Alfalfa Forage Yield and Nutritive Value in a Mediterranean Climate." *Grassland Research* 2, no. 3: 153–166. https://doi.org/10.1002/glr2.12061.

Aybar, C., W. Lavado, E. Sabino, S. Ramírez, J. Huerta, and O. Felipe-Obando. 2017. *Atlas de zonas de vida del Perú: Guía Explicativa*. Servicio Nacional de Meteorología e Hidrología del Perú. https://www.senamhi.gob.pe/load/file/01402SENA-9.pdf.

Bai, G., F. He, G. Shan, et al. 2024. "Effect of Saline Irrigation Water on Alfalfa Growth and Development in Saline–Alkali Soils." *Agronomy* 14, no. 12: 2790. https://doi.org/10.3390/agronomy14122790.

Banks, D., H. Markland, P. V. Smith, et al. 2004. "Distribution, Salinity and pH Dependence of Elements in Surface Waters of the Catchment Areas of the Salars of Coipasa and Uyuni, Bolivian Altiplano." *Journal of Geochemical Exploration* 84, no. 3: 141–166. https://doi.org/10.1016/j.gexplo.2004.07.001.

Bedolla-Rivera, H. I., M. d. L. X. Negrete-Rodríguez, M. d. R. Medina-Herrera, et al. 2022. "Comparison of Methodologies of Soil Quality Indices (SQI) for Monitoring Soil Remediation Under Biosolid Amendments." *Revista Internacional de Contaminación Ambiental* 38: 1–17. https://doi.org/10.20937/RICA.54449.

Bello, S. K., A. H. Alayafi, S. G. AL-Solaimani, and K. A. M. Abo-Elyousr. 2021. "Mitigating Soil Salinity Stress With Gypsum and Bio-Organic Amendments: A Review." *Agronomy* 11, no. 9: 1735. https://doi.org/10.3390/agronomy11091735.

Bernal, R. E. 2013. "Informe de Cierre de Proyecto C-09-30 "Desarrollo ganadero lechero y mercadeo de quesos en el corredor Puno, Juliaca y Ayavir" (Nos. 113-PP-GP-2013; p. 13)."

Bi, X., H. Chu, M. Fu, et al. 2023. "Distribution Characteristics of Organic Carbon (Nitrogen) Content, Cation Exchange Capacity, and Specific Surface Area in Different Soil Particle Sizes." *Scientific Reports* 13, no. 1: 12242. https://doi.org/10.1038/s41598-023-38646-0.

Bromberg, F., and D. S. Pérez. 2012. "Interpolación Espacial Mediante Aprendizaje de Máquinas en Viñedos de la Provincia de Mendoza, Argentina. XIII Argentine Symposium on Artificial Intelligence (ASAI 2012) (XLI JAIIO, La Plata, 27 y 28 de agosto de 2012)."

Burrough, P. A., R. A. McDonnell, and C. D. Lloyd. 2015. *Principles of Geographical Information Systems*. OUP Oxford.

Cuellar-Condori, N., S. Mejia, R. Quiñones, et al. 2026. "Spatial Modelling of Soil Quality Index Using Regression–Kriging and Delineation of Nutrient Management Zones in High-Andean Quinoa Fields, Southern Peru." *Agronomy* 16, no. 7: 680. https://doi.org/10.3390/agronomy16070680.

Daba, A. W. 2025. "Rehabilitation of Soil Salinity and Sodicity Using Diverse Amendments and Plants: A Critical Review." *Discover Environment* 3, no. 1: 53. https://doi.org/10.1007/s44274-025-00199-6.

Daba, A. W., and A. S. Qureshi. 2021. "Review of Soil Salinity and Sodicity Challenges to Crop Production in the Lowland Irrigated Areas of Ethiopia and its Management Strategies." *Land* 10, no. 12: 1377. https://doi.org/10.3390/land10121377.

Dash, P. K., B. A. Miller, N. Panigrahi, and A. Mishra. 2024. "Exploring the Effect of Sampling Density on Spatial Prediction With Spatial Interpolation of Multiple Soil Nutrients at a Regional Scale." *Land* 13, no. 10: 1615. https://doi.org/10.3390/land13101615.

De Caires, S. A., C. S. Martin, M. A. Atwell, F. Kaya, G. A. Wuddivira, and M. N. Wuddivira. 2025. "Advancing Soil Mapping and Management Using Geostatistics and Integrated Machine Learning and Remote Sensing Techniques: A Synoptic Review." *Discover Soil* 2, no. 1: 53. https://doi.org/10.1007/s44378-025-00082-z.

Doran, J. W., and T. B. Parkin. 2015. *Defining and Assessing Soil Quality*, edited by J. W. Doran, D. C. Coleman, D. F. Bezdicek, and B. A. Stewart, 1–21. Soil Science Society of America and American Society of Agronomy. https://doi.org/10.2136/sssaspecpub35.c1.

EPA. 2004. "Method 9045D: Soil and Waste pH, Part of Test Methods for Evaluating Solid Waste, Physical/Chemical Methods. Soil Waste PH, 1–5."

Esri. 2020. "Cómo funciona Kriging—ArcGIS Pro | Documentación." https://pro.arcgis.com/es/pro-app/latest/tool-reference/3d-analyst/how-kriging-works.htm.

Estrada-Godoy, F., G. Cruz-Cárdenas, S. Ochoa-Estrada, and J. T. Silva. 2023. "Cartografía Digital de suelos con regresión-Kriging y datos de sensores remotos." *Revista Terra Latinoamericana* 41. https://doi.org/10.28940/terra.v41i0.1617.

FAO. 2024. *Global Map of Salt-Affected Soils*. Food and Agriculture Organization of the United Nations. https://www.fao.org/soils-portal/data-hub/soil-maps-and-databases/global-map-of-salt-affected-soils/en/.

Fernández Villafañez, S. 2022. "Métodos de regresión y clasificación basados en árboles." https://uvadoc.uva.es/handle/10324/53822.

Fick, S. E., and R. J. Hijmans. 2017. "WorldClim 2: New 1-Km Spatial Resolution Climate Surfaces for Global Land Areas." *International Journal of Climatology* 37, no. 12: 4302–4315. https://doi.org/10.1002/joc.5086.

Fu, Y., J. Song, J. Guo, Y. Fu, and Y. Cai. 2024. "Prediction and Analysis of Sea Surface Temperature Based on LSTM-Transformer Model." *Regional Studies in Marine Science* 78: 103726. https://doi.org/10.1016/j.rsma.2024.103726.

Gashi, N., Z. Szőke, A. Czakó, et al. 2025. "Gypsum and Tillage Practices for Combating Soil Salinity and Enhancing Crop Productivity." *Agriculture* 15, no. 6: 658. https://doi.org/10.3390/agriculture15060658.

Green, H., P. Larsen, J. Koci, W. Edwards, and P. N. Nelson. 2023. "Long-Term Effects of Gypsum on the Chemistry of Sodic Soils." *Soil and Tillage Research* 233: 105780. https://doi.org/10.1016/j.still.2023.105780.

Havlin, J. L., S. L. Tisdale, W. D. Nelson, and J. D. Beaton. 2016. *Soil Fertility and Fertilizers: An Introduction to Nutrient Management*. Vol. 8. 6th ed. Pearson Education India. https://www.researchgate.net/profile/Praveen-Kumar-521/publication/366175716_Soil_Fertility_and_Fertilizers_by_John_L_Havlin_z-liborg/links/63948fbde42faa7e75af15db/Soil-Fertility-and-Fertilizers-by-John-L-Havlin-z-liborg.pdf.

Hengl, T., G. B. M. Heuvelink, and D. G. Rossiter. 2007. "About Regression-Kriging: From Equations to Case Studies." *Computers & Geosciences* 33, no. 10: 1301–1315. https://doi.org/10.1016/j.cageo.2007.05.001.

Hengl, T., J. Mendes De Jesus, G. B. M. Heuvelink, et al. 2017. "SoilGrids250m: Global Gridded Soil Information Based on Machine Learning." *PLoS One* 12, no. 2: e0169748. https://doi.org/10.1371/journal.pone.0169748.

Hervé, D., R. Ledezma, and V. Orsag. 2002. "Limitantes y manejo de los suelos salinos y/o sodicos en el Altiplano bolivano." https://www.documentation.ird.fr/hor/fdi:010029752.

IDESEP. 2020. "Mapa de Clasificación Climática del Perú." https://idesep.senamhi.gob.pe/geovisoridesep/go?accion=05.01.001.03.001.512.2021.00.00.

INEI. 2023. "Compendio Estadístico, Puno 2023—Informes y publicaciones—Instituto Nacional de Estadística e Informática—Plataforma del Estado Peruano." https://www.gob.pe/institucion/inei/informes-publicaciones/5373689-compendio-estadistico-puno-2023.

INGEMMET. 2016. "Mapa geomorfológico del Perú [shapefile] [Instituto Geológico, Minero y Metalúrgico]. Geocatmin." https://geocatmin.ingemmet.gob.pe/geocatmin/.

ISO. 1994. "ISO 11265:1994, Soil Quality—Determination of Specific Electrical Conductivity. ISO 11265." https://www.iso.org/es/contents/data/standard/01/92/19243.html.

ISO. 2006. "ISO 11464:2006, Soil Quality—Pretreatment of Samples for Physico-Chemical Analysis. ISO." https://www.iso.org/standard/37718.html.

ISRIC-World Soil. 2025. "SoilGrids250m 2.0. SoilGrids Web Portal." https://soilgrids.org/.

IUSS Working Group WRB. 2024. *World Reference Base for Soil Resources. International Soil Classification System for Naming Soils and Creating Legends for Soil Maps*. LCC MAKS Press. https://doi.org/10.29003/m4174.978-5-317-07235-3.

Jalane, O. I., J. M. Mafalacusser, E. V. Da Siva, and A. S. A. Mabjaia. 2024. "Geoestadística y SIG Como Técnica de Mapeamientos de las Propriedades Químicas del suelo." *Revista Angolana de Ciencias* 5, no. 2: e050208. https://doi.org/10.54580/R0502.08.

Kargas, G., P. Londra, and K. Sotirakoglou. 2022. "The Effect of Soil Texture on the Conversion Factor of 1:5 Soil/Water Extract Electrical Conductivity (EC1:5) to Soil Saturated Paste Extract Electrical Conductivity (ECe)." *Water* 14, no. 4: 642.

Martínez, C. R. 2020. "Modelado geoestadístico de fertilidad de un terreno agrícola mediante mapas de Kriging que interpolan los datos de análisis químico de suelos." *Producción Agropecuaria y Desarrollo Sostenible* 9: 63–84. https://doi.org/10.5377/payds.v9i0.11858.

Mitsuta, A., K. S. Lourenço, B. G. De Oliveira, O. Y. De Assis Costa, H. Cantarella, and E. E. Kuramae. 2025. "Soil pH Determines the Shift of Key Microbial Energy Metabolic Pathways Associated With Soil Nutrient Cycle." *Applied Soil Ecology* 208: 105992. https://doi.org/10.1016/j.apsoil.2025.105992.

Mohanavelu, A., S. R. Naganna, and N. Al-Ansari. 2021. "Irrigation Induced Salinity and Sodicity Hazards on Soil and Groundwater: An Overview of Its Causes, Impacts and Mitigation Strategies." *Agriculture* 11, no. 10: 983. https://doi.org/10.3390/agriculture11100983.

Morsy, S., I. S. Elbasyoni, S. Baenziger, and A. M. Abdallah. 2022. "Gypsum Amendment Influences Performance and Mineral Absorption in Wheat Cultivars Grown in Normal and Saline-Sodic Soils." *Journal of Agronomy and Crop Science* 208, no. 5: 675–692. https://doi.org/10.1111/jac.12598.

Niaz, S., J. B. Wehr, R. C. Dalal, P. M. Kopittke, and N. W. Menzies. 2022. "Organic Amendments and Gypsum Reduce Dispersion and Increase Aggregation of Two Sodic Vertisols." *Geoderma* 425: 116047. https://doi.org/10.1016/j.geoderma.2022.116047.

Niaz, S., J. B. Wehr, R. C. Dalal, P. M. Kopittke, and N. W. Menzies. 2023. "Wetting and Drying Cycles, Organic Amendments, and Gypsum Play a

Key Role in Structure Formation and Stability of Sodic Vertisols." *Soil* 9, no. 1: 141–154. https://doi.org/10.5194/soil-9-141-2023.

NOM-021-RECNAT-2000. 2002. "NOM-021-RECNAT-2000. Natural Resources and Environment Secretary. Mexican Official Standard. Specifications of Fertility, Salinity, and Soil Classification. Study, Sampling and Analysis. Diario Oficial." https://www.ordenjuridico.gob.mx/Documentos/Federal/wo69255.pdf.

Noonari, A. R., B. A. Nindwani, A. Tunio, et al. 2025. "Role of Gypsum in Reclaiming Saline-Sodic Soils to Improving Soil Health and Enhancing Productivity." *Journal of Agriculture and Biology* 3, no. 1: 46–56. https://doi.org/10.55627/agribiol.003.01.1091.

Odeha, I. O. A., A. B. McBratney, and D. J. Chittleborough. 1994. "Spatial Prediction of Soil Properties From Landform Attributes Derived From a Digital Elevation Model." *Geoderma* 63, no. 3–4: 197–214. https://doi.org/10.1016/0016-7061(94)90063-9.

Oster, J. D., I. Shainberg, and I. P. Abrol. 2015. "Reclamation of Salt-Affected Soils." In *Agronomy Monographs*, edited by R. W. Skaggs and J. Van Schilfgaarde, 659–691. American Society of Agronomy, Crop Science Society of America, Soil Science Society of America. https://doi.org/10.2134/agronmonogr38.c19.

Ozlu, E., G. Gozukara, M. Acar, S. Bilen, and E. Babur. 2022. "Field-Scale Evaluation of the Soil Quality Index as Influenced by Dairy Manure and Inorganic Fertilizers." *Sustainability* 14, no. 13: 7593. https://doi.org/10.3390/su14137593.

Pásztor, L., K. Z. Szabó, G. Szatmári, A. Laborczi, and Á. Horváth. 2016. "Mapping Geogenic Radon Potential by Regression Kriging." *Science of the Total Environment* 544: 883–891. https://doi.org/10.1016/j.scitotenv.2015.11.175.

Perez-Zapata, J., L. Delgado-Bejarano, J. Osorio-Cardona, M. Bernal-Monterrosa, and S. Zapata-Henao. 2024. "Variabilidad espacial de propiedades fisicoquímicas en suelos bananeros de Urabá-Colombia." *Acorbat Revista de Tecnología y Ciencia/Acorbat Journal of Technology and Science* 1, no. 1: 7. https://doi.org/10.62498/ARTC.2407.

Poma-Chamana, R., C. Vilca-Gamarra, N. Hermoza, et al. 2025. "Estimation and Mapping of Soil Fertility Index in Arid Agricultural Environments of the Tambo Valley Using Regression Kriging." *Frontiers in Soil Science* 5: 1706974.

Programa de Desarrollo Productivo Agrario Rural. 2018. *Manual De Abonamiento Con Guano De Las Islas (Agro Rural – Dirección de Abonos)*. Digital Print Service.

Qadir, M., and S. Schubert. 2002. "Degradation Processes and Nutrient Constraints in Sodic Soils." *Land Degradation & Development* 13, no. 4: 275–294. https://doi.org/10.1002/ldr.504.

Quispe, K., N. Hermoza, S. Mejia, et al. 2025. "Spatial Analysis of Soil Acidity and Available Phosphorus in Coffee-Growing Areas of Pichanaqui: Implications for Liming and Site-Specific Fertilization." *Agriculture* 15, no. 15: 1632.

Quispe, K., S. Mejía, C. Carbajal, L. Alejandro, P. Verástegui, and R. Solórzano. 2024. "Spatial Variability of Soil Acidity and Lime Requirements for Potato Cultivation in the Huánuco Highlands." *Agriculture* 14, no. 12: 2286.

Rengasamy, P. 2002. "Transient Salinity and Subsoil Constraints to Dryland Farming in Australian Sodic Soils: An Overview." *Australian Journal of Experimental Agriculture* 42, no. 3: 351–361. https://doi.org/10.1071/EA01111.

Rengasamy, P. 2010. "Soil Processes Affecting Crop Production in Salt-Affected Soils." *Functional Plant Biology* 37, no. 7: 613–620. https://doi.org/10.1071/FP09249.

Rengasamy, P., E. Tavakkoli, and G. K. McDonald. 2016. "Exchangeable Cations and Clay Dispersion: Net Dispersive Charge, a New Concept for Dispersive Soil." *European Journal of Soil Science* 67, no. 5: 659–665. https://doi.org/10.1111/ejss.12369.

Revollo, M. M. 2001. "Management Issues in the Lake Titicaca and Lake Poopo System: Importance of Developing a Water Budget." *Lakes & Reservoirs: Science, Policy and Management for Sustainable Use* 6, no. 3: 225–229. https://doi.org/10.1046/j.1440-1770.2001.00151.x.

Roberton, S. D., J. M. Bennett, C. R. Lobsey, and T. F. Bishop. 2020. "Assessing the Sensitivity of Site-Specific Lime and Gypsum Recommendations to Soil Sampling Techniques and Spatial Density of Data Collection in Australian Agriculture: A Pedometric Approach." *Agronomy* 10, no. 11: 1676. https://doi.org/10.3390/agronomy10111676.

Shahid, S. A., M. Zaman, and L. Heng. 2018. "Introduction to Soil Salinity, Sodicity and Diagnostics Techniques." In *Guideline for Salinity Assessment, Mitigation and Adaptation Using Nuclear and Related Techniques*, edited by M. Zaman, S. A. Shahid, and L. Heng, 1–42. Springer International Publishing. https://doi.org/10.1007/978-3-319-96190-3_1.

Shi, H. 2022. "To Reduce Soil Salinity: The Role of Irrigation and Water Management in Global Arid Regions Across Development Phases (Version 1). arXiv." https://doi.org/10.48550/ARXIV.2204.02029.

Singh, Y. P., S. Arora, V. K. Mishra, and A. K. Singh. 2023. "Rationalizing Mineral Gypsum Use Through Microbially Enriched Municipal Solid Waste Compost for Amelioration and Regaining Productivity Potential of Degraded Alkali Soils." *Scientific Reports* 13, no. 1: 11816. https://doi.org/10.1038/s41598-023-37823-5.

Stavi, I., N. Thevs, and S. Priori. 2021. "Soil Salinity and Sodicity in Drylands: A Review of Causes, Effects, Monitoring, and Restoration Measures." *Frontiers in Environmental Science* 9: 712831. https://doi.org/10.3389/fenvs.2021.712831.

Tian, Y., W. Jiang, G. Chen, X. Wang, and T. Li. 2024. "Gypsum and Organic Materials Improved Soil Quality and Crop Production in Saline-Alkali on the Loess Plateau of China." *Frontiers in Environmental Science* 12: 1434147. https://doi.org/10.3389/fenvs.2024.1434147.

Villatoro, M., C. Henríquez, and F. Sancho. 2008. "Comparación de los interpoladores IDW y Kriging en la variación espacial de pH, Ca, CICE y P del suelo." *Agronomía Costarricense* 32: 95–105. https://doi.org/10.15517/rac.v32i1.6773.

Vista, S. P., Y. K. Gaihre, and K. R. Dahal. 2024. "Plant Nutrient Availability in Acid Soil and Management Strategies." In *Climate Change and Soil-Water-Plant Nexus*, edited by M. M. Rahman, J. C. Biswas, and R. S. Meena, 331–353. Springer Nature Singapore. https://doi.org/10.1007/978-981-97-6635-2_11.

Wickham, H. 2016. *Ggplot2: Elegant Graphics for Data Analysis*. Springer International Publishing.

Xu, Y., Z. Liu, Z. Shen, et al. 2024. "Alfalfa With Forage Crop Rotation Alleviates Continuous Alfalfa Obstacles Through Regulating Soil Enzymes and Bacterial Community Structures." *Agronomy* 14, no. 7: 1349. https://doi.org/10.3390/agronomy14071349.

Yang, F., F. An, H. Ma, Z. Wang, X. Zhou, and Z. Liu. 2016. "Variations on Soil Salinity and Sodicity and Its Driving Factors Analysis Under Microtopography in Different Hydrological Conditions." *Water* 8, no. 6: 227. https://doi.org/10.3390/w8060227.

Supporting Information

Additional supporting information can be found online in the Supporting Information section. **Figure S1:** (a) Average Temperature and (b) Average Precipitation in Ayaviri District, (c) Average Temperature and (d) Average Precipitation in Macari District. **Figure S2:** (a) Predominant geomorphology, (b) Soil taxonomic categories, (c) Classification of life zones and (d) Predominant crops in the districts of Ayaviri and Macari.